The $\eta_c(2980)$ formation in two-photon collisions at LEP energies

J. Abdallah, P. Abreu, W. Adam, P. Adzic, T. Albrecht, T. Alderweireld, R. Alemany-Fernandez, T. Allmendinger, P.P. Allport, U. Amaldi, et al.

EUROPEAN ORGANIZATION FOR NUCLEAR RESEARCH

CERN–EP/2003-035

22 Mai 2003

The $\eta_c(2980)$ formation in two-photon collisions at LEP energies

DELPHI Collaboration

Abstract

$\eta_c(2980)$ production in $\gamma\gamma$ interactions has been detected via its decays into $K^0_s K^{\pm}\pi^{\mp}$, $K^+K^-K^+K^-$ and $K^+K^-\pi^+\pi^-$ in the data taken with the DELPHI detector at LEP1 and LEP2 energies. The two-photon radiative width averaged over all observed decay channels is $\Gamma_{\gamma\gamma} = 13.9 \pm 2.0$ (stat.) $\pm$ 1.4(syst.) $\pm$ 2.7 (BR) keV. No direct decay channel $\eta_c \to \pi^+\pi^-\pi^+\pi^-$ has been observed. An upper limit $\Gamma_{\gamma\gamma} < 5.5$ keV at 95% confidence level has been evaluated for this decay mode.

(Accepted by Eur. Phys. J. C)

J.Abdallah[25], P.Abreu[22], W.Adam[51], P.Adzic[11], T.Albrecht[17], T.Alderweireld[2], R.Alemany-Fernandez[8], T.Allmendinger[17], P.P.Allport[23], U.Amaldi[29], N.Amapane[45], S.Amato[48], E.Anashkin[36], A.Andreazza[28], S.Andringa[22], N.Anjos[22], P.Antilogus[27], W-D.Apel[17], Y.Arnoud[14], S.Ask[26], B.Asman[44], J.E.Augustin[25], A.Augustinus[8], P.Baillon[8], A.Ballestrero[46], P.Bambade[20], R.Barbier[27], D.Bardin[16], G.Barker[17], A.Baroncelli[39], M.Battaglia[8], M.Baubillier[25], K-H.Becks[53], M.Begalli[6], A.Behrmann[53], E.Ben-Haim[20], N.Benekos[32], A.Benvenuti[5], C.Berat[14], M.Berggren[25], L.Berntzon[44], D.Bertrand[2], M.Besancon[40], N.Besson[40], D.Bloch[9], M.Blom[31], M.Bluj[52], M.Bonesini[29], M.Boonekamp[40], P.S.L.Booth[23], G.Borisov[21], O.Botner[49], B.Bouquet[20], T.J.V.Bowcock[23], I.Boyko[16], M.Bracko[43], R.Brenner[49], E.Brodet[35], P.Bruckman[18], J.M.Brunet[7], L.Bugge[33], P.Buschmann[53], M.Calvi[29], T.Camporesi[8], V.Canale[38], F.Carena[8], N.Castro[22], F.Cavallo[5], M.Chapkin[42], Ph.Charpentier[8], P.Checchia[36], R.Chierici[8], P.Chliapnikov[42], J.Chudoba[8], S.U.Chung[8], K.Cieslik[18], P.Collins[8], R.Contri[13], G.Cosme[20], F.Cossutti[47], M.J.Costa[50], B.Crawley[1], D.Crennell[37], J.Cuevas[34], J.D'Hondt[2], J.Dalmau[44], T.da Silva[48], W.Da Silva[25], G.Della Ricca[47], A.De Angelis[47], W.De Boer[17], C.De Clercq[2], B.De Lotto[47], N.De Maria[45], A.De Min[36], L.de Paula[48], L.Di Ciaccio[38], A.Di Simone[39], K.Doroba[52], J.Drees[53,8], M.Dris[32], G.Eigen[4], T.Ekelof[49], M.Ellert[49], M.Elsing[8], M.C.Espirito Santo[22], G.Fanourakis[11], D.Fassouliotis[11,3], M.Feindt[17], J.Fernandez[41], A.Ferrer[50], F.Ferro[13], U.Flagmeyer[53], H.Foeth[8], E.Fokitis[32], F.Fulda-Quenzer[20], J.Fuster[50], M.Gandelman[48], C.Garcia[50], Ph.Gavillet[8], E.Gazis[32], R.Gokieli[8,52], B.Golob[43], G.Gomez-Ceballos[41], P.Goncalves[22], E.Graziani[39], G.Grosdidier[20], K.Grzelak[52], J.Guy[37], C.Haag[17], A.Hallgren[49], K.Hamacher[53], K.Hamilton[35], J.Hansen[33], S.Haug[33], F.Hauler[17], V.Hedberg[26], M.Hennecke[17], H.Herr[8], J.Hoffman[52], S-O.Holmgren[44], P.J.Holt[8], M.A.Houlden[23], K.Hultqvist[44], J.N.Jackson[23], G.Jarlskog[26], P.Jarry[40], D.Jeans[35], E.K.Johansson[44], P.D.Johansson[44], P.Jonsson[27], C.Joram[8], L.Jungermann[17], F.Kapusta[25], S.Katsanevas[27], E.Katsoufis[32], G.Kernel[43], B.P.Kersevan[8,43], A.Kiiskinen[15], B.T.King[23], N.J.Kjaer[8], P.Kluit[31], P.Kokkinias[11], C.Kourkoumelis[3], O.Kouznetsov[16], Z.Krumstein[16], M.Kucharczyk[18], J.Lamsa[1], G.Leder[51], F.Ledroit[14], L.Leinonen[44], R.Leitner[30], J.Lemonne[2], V.Lepeltier[20], T.Lesiak[18], W.Liebig[53], D.Liko[51], A.Lipniacka[44], J.H.Lopes[48], J.M.Lopez[34], D.Loukas[11], P.Lutz[40], L.Lyons[35], J.MacNaughton[51], A.Malek[53], S.Maltezos[32], F.Mandl[51], J.Marco[41], R.Marco[41], B.Marechal[48], M.Margoni[36], J-C.Marin[8], C.Mariotti[8], A.Markou[11], C.Martinez-Rivero[41], J.Masik[12], N.Mastroyiannopoulos[11], F.Matorras[41], C.Matteuzzi[29], F.Mazzucato[36], M.Mazzucato[36], R.Mc Nulty[23], C.Meroni[28], W.T.Meyer[1], E.Migliore[45], W.Mitaroff[51], U.Mjoernmark[26], T.Moa[44], M.Moch[17], K.Moenig[8,10], R.Monge[13], J.Montenegro[31], D.Moraes[48], S.Moreno[22], P.Morettini[13], U.Mueller[53], K.Muenich[53], M.Mulders[31], L.Mundim[6], W.Murray[37], B.Muryn[19], G.Myatt[35], T.Myklebust[33], M.Nassiakou[11], F.Navarria[5], K.Nawrocki[52], R.Nicolaidou[40], M.Nikolenko[16,9], A.Oblakowska-Mucha[19], V.Obraztsov[42], A.Olshevski[16], A.Onofre[22], R.Orava[15], K.Osterberg[15], A.Ouraou[40], A.Oyanguren[50], M.Paganoni[29], S.Paiano[5], J.P.Palacios[23], H.Palka[18], Th.D.Papadopoulou[32], L.Pape[8], C.Parkes[24], F.Parodi[13], U.Parzefall[8], A.Passeri[39], O.Passon[53], L.Peralta[22], V.Perepelitsa[50], A.Perrotta[5], A.Petrolini[13], J.Piedra[41], L.Pieri[39], F.Pierre[40], M.Pimenta[22], E.Piotto[8], T.Podobnik[43], V.Poireau[8], M.E.Pol[6], G.Polok[18], P.Poropat[†47], V.Pozdniakov[16], N.Pukhaeva[2,16], A.Pullia[29], J.Rames[12], L.Ramler[17], A.Read[33], P.Rebecchi[8], J.Rehn[17], D.Reid[31], R.Reinhardt[53], P.Renton[35], F.Richard[20], J.Ridky[12], M.Rivero[41], D.Rodriguez[41], A.Romero[45], P.Ronchese[36], E.Rosenberg[1], P.Roudeau[20], T.Rovelli[5], V.Ruhlmann-Kleider[40], D.Ryabtchikov[42], A.Sadovsky[16], L.Salmi[15], J.Salt[50], A.Savoy-Navarro[25], U.Schwickerath[8], A.Segar[35], R.Sekulin[37], M.Siebel[53], A.Sisakian[16], G.Smadja[27], O.Smirnova[26], A.Sokolov[42], A.Sopczak[21], R.Sosnowski[52], T.Spassov[8], M.Stanitzki[17], A.Stocchi[20], J.Strauss[51], B.Stugu[4], M.Szczekowski[52], M.Szeptycka[52], T.Szumlak[19], T.Tabarelli[29], A.C.Taffard[23], F.Tegenfeldt[49], J.Timmermans[31], L.Tkatchev[16], M.Tobin[23], S.Todorovova[12], B.Tome[22], A.Tonazzo[29], P.Tortosa[50], P.Travnicek[12], D.Treille[8], G.Tristram[7], M.Trochimczuk[52], C.Troncon[28], M-L.Turluer[40], I.A.Tyapkin[16], P.Tyapkin[16], S.Tzamarias[11], V.Uvarov[42], G.Valenti[5], P.Van Dam[31], J.Van Eldik[8], A.Van Lysebetten[2], N.van Remortel[2], I.Van Vulpen[8], G.Vegni[28], F.Veloso[22], W.Venus[37], F.Verbeure[2], P.Verdier[27], V.Verzi[38], D.Vilanova[40], L.Vitale[47], V.Vrba[12], H.Wahlen[53], A.J.Washbrook[23], C.Weiser[17],

D.Wicke[8], J.Wickens[2], G.Wilkinson[35], M.Winter[9], M.Witek[18], O.Yushchenko[42], A.Zalewska[18], P.Zalewski[52], D.Zavrtanik[43], V.Zhuravlov[16], N.I.Zimin[16], A.Zintchenko[16], M.Zupan[11]

[1]Department of Physics and Astronomy, Iowa State University, Ames IA 50011-3160, USA
[2]Physics Department, Universiteit Antwerpen, Universiteitsplein 1, B-2610 Antwerpen, Belgium
and IIHE, ULB-VUB, Pleinlaan 2, B-1050 Brussels, Belgium
and Faculté des Sciences, Univ. de l'Etat Mons, Av. Maistriau 19, B-7000 Mons, Belgium
[3]Physics Laboratory, University of Athens, Solonos Str. 104, GR-10680 Athens, Greece
[4]Department of Physics, University of Bergen, Allégaten 55, NO-5007 Bergen, Norway
[5]Dipartimento di Fisica, Università di Bologna and INFN, Via Irnerio 46, IT-40126 Bologna, Italy
[6]Centro Brasileiro de Pesquisas Físicas, rua Xavier Sigaud 150, BR-22290 Rio de Janeiro, Brazil
and Depto. de Física, Pont. Univ. Católica, C.P. 38071 BR-22453 Rio de Janeiro, Brazil
and Inst. de Física, Univ. Estadual do Rio de Janeiro, rua São Francisco Xavier 524, Rio de Janeiro, Brazil
[7]Collège de France, Lab. de Physique Corpusculaire, IN2P3-CNRS, FR-75231 Paris Cedex 05, France
[8]CERN, CH-1211 Geneva 23, Switzerland
[9]Institut de Recherches Subatomiques, IN2P3 - CNRS/ULP - BP20, FR-67037 Strasbourg Cedex, France
[10]Now at DESY-Zeuthen, Platanenallee 6, D-15735 Zeuthen, Germany
[11]Institute of Nuclear Physics, N.C.S.R. Demokritos, P.O. Box 60228, GR-15310 Athens, Greece
[12]FZU, Inst. of Phys. of the C.A.S. High Energy Physics Division, Na Slovance 2, CZ-180 40, Praha 8, Czech Republic
[13]Dipartimento di Fisica, Università di Genova and INFN, Via Dodecaneso 33, IT-16146 Genova, Italy
[14]Institut des Sciences Nucléaires, IN2P3-CNRS, Université de Grenoble 1, FR-38026 Grenoble Cedex, France
[15]Helsinki Institute of Physics, P.O. Box 64, FIN-00014 University of Helsinki, Finland
[16]Joint Institute for Nuclear Research, Dubna, Head Post Office, P.O. Box 79, RU-101 000 Moscow, Russian Federation
[17]Institut für Experimentelle Kernphysik, Universität Karlsruhe, Postfach 6980, DE-76128 Karlsruhe, Germany
[18]Institute of Nuclear Physics,Ul. Kawiory 26a, PL-30055 Krakow, Poland
[19]Faculty of Physics and Nuclear Techniques, University of Mining and Metallurgy, PL-30055 Krakow, Poland
[20]Université de Paris-Sud, Lab. de l'Accélérateur Linéaire, IN2P3-CNRS, Bât. 200, FR-91405 Orsay Cedex, France
[21]School of Physics and Chemistry, University of Lancaster, Lancaster LA1 4YB, UK
[22]LIP, IST, FCUL - Av. Elias Garcia, 14-1^o, PT-1000 Lisboa Codex, Portugal
[23]Department of Physics, University of Liverpool, P.O. Box 147, Liverpool L69 3BX, UK
[24]Dept. of Physics and Astronomy, Kelvin Building, University of Glasgow, Glasgow G12 8QQ
[25]LPNHE, IN2P3-CNRS, Univ. Paris VI et VII, Tour 33 (RdC), 4 place Jussieu, FR-75252 Paris Cedex 05, France
[26]Department of Physics, University of Lund, Sölvegatan 14, SE-223 63 Lund, Sweden
[27]Université Claude Bernard de Lyon, IPNL, IN2P3-CNRS, FR-69622 Villeurbanne Cedex, France
[28]Dipartimento di Fisica, Università di Milano and INFN-MILANO, Via Celoria 16, IT-20133 Milan, Italy
[29]Dipartimento di Fisica, Univ. di Milano-Bicocca and INFN-MILANO, Piazza della Scienza 2, IT-20126 Milan, Italy
[30]IPNP of MFF, Charles Univ., Areal MFF, V Holesovickach 2, CZ-180 00, Praha 8, Czech Republic
[31]NIKHEF, Postbus 41882, NL-1009 DB Amsterdam, The Netherlands
[32]National Technical University, Physics Department, Zografou Campus, GR-15773 Athens, Greece
[33]Physics Department, University of Oslo, Blindern, NO-0316 Oslo, Norway
[34]Dpto. Fisica, Univ. Oviedo, Avda. Calvo Sotelo s/n, ES-33007 Oviedo, Spain
[35]Department of Physics, University of Oxford, Keble Road, Oxford OX1 3RH, UK
[36]Dipartimento di Fisica, Università di Padova and INFN, Via Marzolo 8, IT-35131 Padua, Italy
[37]Rutherford Appleton Laboratory, Chilton, Didcot OX11 OQX, UK
[38]Dipartimento di Fisica, Università di Roma II and INFN, Tor Vergata, IT-00173 Rome, Italy
[39]Dipartimento di Fisica, Università di Roma III and INFN, Via della Vasca Navale 84, IT-00146 Rome, Italy
[40]DAPNIA/Service de Physique des Particules, CEA-Saclay, FR-91191 Gif-sur-Yvette Cedex, France
[41]Instituto de Fisica de Cantabria (CSIC-UC), Avda. los Castros s/n, ES-39006 Santander, Spain
[42]Inst. for High Energy Physics, Serpukov P.O. Box 35, Protvino, (Moscow Region), Russian Federation
[43]J. Stefan Institute, Jamova 39, SI-1000 Ljubljana, Slovenia and Laboratory for Astroparticle Physics,
Nova Gorica Polytechnic, Kostanjeviska 16a, SI-5000 Nova Gorica, Slovenia,
and Department of Physics, University of Ljubljana, SI-1000 Ljubljana, Slovenia
[44]Fysikum, Stockholm University, Box 6730, SE-113 85 Stockholm, Sweden
[45]Dipartimento di Fisica Sperimentale, Università di Torino and INFN, Via P. Giuria 1, IT-10125 Turin, Italy
[46]INFN,Sezione di Torino, and Dipartimento di Fisica Teorica, Università di Torino, Via P. Giuria 1,
IT-10125 Turin, Italy
[47]Dipartimento di Fisica, Università di Trieste and INFN, Via A. Valerio 2, IT-34127 Trieste, Italy
and Istituto di Fisica, Università di Udine, IT-33100 Udine, Italy
[48]Univ. Federal do Rio de Janeiro, C.P. 68528 Cidade Univ., Ilha do Fundão BR-21945-970 Rio de Janeiro, Brazil
[49]Department of Radiation Sciences, University of Uppsala, P.O. Box 535, SE-751 21 Uppsala, Sweden
[50]IFIC, Valencia-CSIC, and D.F.A.M.N., U. de Valencia, Avda. Dr. Moliner 50, ES-46100 Burjassot (Valencia), Spain
[51]Institut für Hochenergiephysik, Österr. Akad. d. Wissensch., Nikolsdorfergasse 18, AT-1050 Vienna, Austria
[52]Inst. Nuclear Studies and University of Warsaw, Ul. Hoza 69, PL-00681 Warsaw, Poland
[53]Fachbereich Physik, University of Wuppertal, Postfach 100 127, DE-42097 Wuppertal, Germany
† deceased

1 Introduction

Among $\gamma\gamma$ induced final states, those with exclusive meson resonance production play an important role, since the measurement of the production cross-section and the corresponding radiative width provide information on the quark-gluon structure of the investigated particle. Among these final states, those with mesons built up of heavy quarks are particularly interesting since such mesons can be described with nonrelativistic models. In particular, a precise measurement of the two-photon partial width for charmonium states would provide valuable information on QCD corrections to $c\bar{c}$ quarkonium.

The very first estimations of the η_c partial width, $\Gamma_{\gamma\gamma}(\eta_c)$, were obtained from its ratios to the known widths for $\psi \to \mu^+\mu^-$ and $\eta_c \to gg$ giving values of 8 keV and 4 keV respectively [1]. Different models and corrections were applied to them later, giving values from 3 to 14 keV, see [2] and references therein. An even bigger discrepancy is observed between values obtained by numerous experimental groups. Among them there are many experiments where two interacting photons radiated by electron and positron beams couple to this resonant state, [3]- [12]. The results for $\Gamma_{\gamma\gamma}(\eta_c)$ range from 4 keV to 27 keV.

In this paper we report on the production and decays of the η_c resonance using data collected by the DELPHI detector during the period 1994-1999 corresponding to a range of centre-of-mass energies from 90 GeV up to 202 GeV and an integrated luminosity of $\mathcal{L} = 531$ pb^{-1}. The aim of this analysis was to determine the radiative width of the η_c resonance separately for each decay channel, using the production process:

$$e^+e^- \to e^+e^-\eta_c(2980) \tag{1}$$

on four-body final states where a distinct signal of the η_c resonance has been observed. To increase the sensitivity for η_c production, we do not require information on the polar angle of the scattered electrons (no tag mode). The superiority of LEP with respect to previous experiments is the higher energy and resulting higher production cross-section for this reaction.

We have analysed the following exclusive final states:

$$\eta_c \to K_s^0 K^\pm \pi^\mp \tag{2}$$

$$\eta_c \to K^+K^-K^+K^- \tag{3}$$

$$\eta_c \to K^+K^-\pi^+\pi^- \tag{4}$$

$$\eta_c \to \pi^+\pi^-\pi^+\pi^- \tag{5}$$

2 Detector

A general description of the DELPHI detector can be found elsewhere [13]. The main features relevant to this analysis are particle tracking and identification. Due to the low momenta of the decay products, their identification is based on measurement of ionization losses (dE/dx) in the Time Projection Chamber (TPC). The particle momenta are determined from track reconstruction and make use of the Vertex Detector, the Inner and Outer Detectors and the TPC. The tracks with lower polar angles are reconstructed in Forward Chambers A/B.

The single track trigger efficiency, expressed in terms of transverse track momentum, has an influence on the overall efficiency of final states produced in $\gamma\gamma$ collisions where

the hadrons have rather low momenta. Having four particles in the final state, originating from the decay of a relatively heavy $\eta_c(2980)$ resonance, results in a large trigger efficiency for an event according to the formula:

$$\mathcal{E}_{ev} = 1 - (1 - \epsilon_1) \times (1 - \epsilon_2) \times (1 - \epsilon_3) \times (1 - \epsilon_4) \tag{6}$$

where $\mathcal{E}_{ev}$ is the total trigger efficiency for an event and the ϵ_i is the single track efficiency which depends on the transverse momentum. A brief description of the trigger system is presented in [14,15].

3 General Data Selection

Data were taken only from running periods when the TPC was fully operational thus ensuring good particle identification. There was no requirement on detecting either scattered electron. Candidates for the $\eta_c(2980)$ decay channels (2)-(5) were selected by requiring:

- exactly four charged particle tracks with zero total charge, coming from the primary interaction region or two tracks originating from the primary vertex and two tracks originating from a secondary vertex,
- the track impact parameters measured with respect to the z-axis (beam axis) to be smaller than 10 cm and those measured in the plane perpendicular to the z-axis smaller than 4 cm,
- the momentum of each particle to be larger than 0.1 GeV/c,
- the square of the total transverse momentum, $(\Sigma\vec{p_t})^2$, of charged particles to be less than 1.0 $(\mathrm{GeV/c})^2$,
- each track to pass through the TPC,
- the total detected energy of charged particles to be less than 10 GeV,
- no particles identified as electrons or muons by the standard lepton identification algorithms,
- the track lengths to be longer than 30 cm,
- the total energy deposit in the electromagnetic calorimeter from neutral particles to be less than 3 GeV,
- the charged particles to have polar angles between 20° and 160°.

Additional criteria which are specific to particular channels are discussed in the next section.

All experimental requirements used in the analyses presented below were chosen to be the same for all data sets corresponding to various beam energies.

4 Analysis

In $\gamma\gamma$ events almost all the available energy and momentum is carried away by the electron and positron which are scattered at very small angles. Therefore the $(\Sigma\vec{p_t})^2$ distribution of the hadronic system is peaked at low values, as shown in Fig.1. To suppress background events which do not originate from $\gamma\gamma$ collisions, the total transverse momentum squared of hadrons in the exclusive process (1) should be smaller than 0.04 $(\mathrm{GeV/c})^2$.

In order to calculate the acceptance and detection efficiency, a Monte Carlo generation program has been used, with the full kinematics of a system produced in $\gamma\gamma$ interactions. All kinematical variables necessary for the description of the two-photon processes were generated using algorithms taken from the package described in [16]. The matrix element, factorized into the flux of quasi-real transverse photons and a covariant amplitude describing both the two-photon η_c production and its decay, has been implemented [17]. For a better understanding of the η_c four pion decay mode we have also determined the efficiency for $\eta_c \to \rho^0\rho^0 \to \pi^+\pi^-\pi^+\pi^-$ with a specific symmetrized matrix element [17]. The Monte Carlo generated events were passed through the standard DELPHI detector simulation procedure [13].

An additional factor contributing to the overall efficiency comes from the trigger acceptance. The trigger simulation following the cuts used for η_c selection in the real data has been applied to events after detector simulation. An event was accepted according to a weight calculated on the basis of the single track efficiency, parameterized as a function of the transverse momentum, p_t, and ranges from 20% for p_t= 0.5 GeV/c to about 95% at p_t= 2 GeV/c [14,15]. Owing to the relatively large mass of the η_c resonant state, the overall trigger efficiency per event was about 90% for channels with pions and about 85% for the $K^+K^-K^+K^-$ final state.

The total efficiency was calculated bin-by-bin in invariant mass by comparing the generated invariant mass distribution with that obtained from the detector simulation after the selection cuts and trigger acceptance. The efficiency for each decay mode as a function of the invariant mass is shown in Fig.2. It should be noted that particle identification was essential for all the channels analysed and was based on dE/dx energy loss measurements [13].

4.1 $\eta_c \to K^0_s K^\pm \pi^\mp$

For the decay chain $\eta_c \to K^0_s K^\pm \pi^\mp \to \pi^+\pi^- K^\pm \pi^\mp$ the $K^0_s \to \pi^+\pi^-$ decay is identified by taking advantage of the relatively large K^0_s decay length ($c\tau$ = 2.68 cm). Therefore, candidates for this decay mode had to have one secondary vertex reconstructed using an algorithm which takes pairs of oppositely charged particle tracks, intersecting them and determining a secondary vertex. Both momenta are recalculated with respect to the new decay vertex and an invariant mass is computed. The resulting K^0_s candidate mass distribution is shown in Fig.3, where clear evidence of a K^0_s signal is seen. Only events with an invariant mass of the two pion candidates, originating from the secondary vertex, in the range from 0.45 GeV/c^2 to 0.55 GeV/c^2 have been taken for further analysis. Of the other two particles which originate from primary interaction region, one is identified as a kaon in 80% of the events selected with one secondary vertex. Hence the crucial criterion for this decay final state selection is the reconstruction of the K^0_s decay vertex.

4.2 $\eta_c \to K^+K^-K^+K^-$

Additional requirements for this decay channel are that at least three particles must be identified as charged kaons and there are no secondary vertices. Only kaons with the probability of identification greater then 0.5 were considered. The dE/dx distribution for all identified particles after the general data selection is plotted in Fig.4 with an insert for the distribution of those originating from η_c (2850 MeV/c^2 $< M(K^+K^-K^+K^-) <$ 3150 MeV/c^2). For events from this η_c mass region, points originating from the rising part of this distribution unquestionably correspond to kaons whereas the horizontal part

may also contain pions from background events and kaons from signal.
A scatter plot (not shown) of the invariant mass of K^+K^- combinations does not indicate any intermediate $\phi\phi$ state. From a fit to the invariant mass distribution, the number of signal events is estimated to be about 46.

Since the average particle momentum is particularly low in this channel, a strong effect could be expected in the invariant mass spectrum resulting from the single track efficiency of the trigger that might produce a fake signal due to the small efficiency at threshold. This has been checked on $\eta_c \to K^+K^-K^+K^-$ events which were generated according to the $\gamma\gamma$ flux (no resonance shape has been assumed) and then decayed according to phase-space. These events were then passed through the trigger and detector simulations. No signal resulting from the trigger activity on the low mass side nor from the experimental cuts on the other was observed in a region of the invariant masses around 3 GeV/c^2, corresponding to the η_c signal. The relatively low background at the $K^+K^-K^+K^-$ invariant mass threshold is explained mostly by the low acceptance and less by the decreased trigger efficiency. The trigger efficiency, as described in previous section turned out to be around 85% at a mass of 3 GeV/c^2.

4.3 $\eta_c \to K^+K^-\pi^+\pi^-$

Given the branching ratio for η_c decay into $K^+K^-\pi^+\pi^-$, BR=2.0±0.7%, and the detector efficiency determined using criteria presented below (Fig.2), a significant signal (of about 4 events per 1 keV of η_c radiative width) would be expected in this channel. In order to select these events it was required that one of the particles was identified as a kaon with probability ≥0.5 and two of the three remaining particles should satisfy selection criteria for pion identification with probability ≥0.5. The identification was based on dE/dx energy losses. All events corresponding to the $K^0_sK^\pm\pi^\mp$ signal, described in section 4.1 have been subtracted from the selected sample. Since the data sample obtained may still contain $K^0_sK^\pm\pi^\mp$ events with no reconstucted secondary vertex, the invariant mass M_{ik} of the two opposite sign particle combinations (excluding the identified kaon) was calculated and events removed if one of the two M_{ik} masses satisfied the condition $|M_{K^0_s} - M_{ik}| < 50$ MeV/c^2. From the data collected by the DELPHI detector during the period mentioned in the first section a signal of about 42 events is obtained.

The intermediate states of $\eta_c \to K^+K^-\pi^+\pi^-$ decay via one or two $K^{*0}(892)$ have not been observed.

4.4 $\eta_c \to \pi^+\pi^-\pi^+\pi^-$

The observation of an $\eta_c \to \pi^+\pi^-\pi^+\pi^-$ decay mode reported by numerous experimental groups remains controversial. This decay has been found by MARK III [4], DM2 [9], TASSO [7] (where the last one did not distinguish between the 4π and the $\rho^0\rho^0$ decay channels). Among more recent experiments this final state has been observed in BES [18]. None of the LEP experiments confirm this decay mode providing only an upper limit [11]. Good particle identification is very important since the $\pi^+\pi^-\pi^+\pi^-$ final state can be confused with the $K^+K^-\pi^+\pi^-$ decay.

In addition to the general selection and the stringent cut on the total transverse momentum, it was also required that all particles were pions with the single track identification probability ≥ 0.5, that only one well reconstructed vertex was found and that each track had to have at least one hit in the Vertex Detector. The final selected sam-

ple consists of ∼3600 events and shows no enhancement around the nominal mass of the η_c resonance, see Fig.5a. Using the PDG values [19] for the η_c parameters, more than 60 events would be expected in this channel. An upper limit of 26 events at 95% confidence limit has been calculated. The above, standard selection criteria lead to an invariant $\pi^+\pi^-\pi^+\pi^-$ mass distribution with a large background that may shadow the signal. Further tightening of the total transverse momentum squared cut from 0.04 to 0.004 $(\mathrm{GeV/c})^2$ and the identification probability from 0.5 to 0.8 reduces the number of observed events to about 600 but still the invariant mass distribution shows no evidence for η_c, see Fig.5b. To avoid a selection bias resulting from the low efficiency for the identification of four pions another selection was performed in which only three particles were identified as pions with probability ≥ 0.5, leaving remaining cuts like in the standard selection, again resulting in no enhancement at η_c invariant mass region, see Fig.5c. A search for the intermediate decay mode, $\rho^0\rho^0$, through an analysis of the two-dimensional plot of the invariant mass of one $\pi^+\pi^-$ system versus that of the remaining $\pi^+\pi^-$ pair has been also performed. Events from the $\rho^0\rho^0$ mass window were selected and used for the calculation of the $\pi^+\pi^-\pi^+\pi^-$ invariant mass spectrum. Since the η_c signal was not seen, these events were attributed to non-resonant $\rho^0\rho^0$ vector mesons production.

5 Results

Experimentally one measures directly the invariant mass ($W_{\gamma\gamma}$) distribution of the $\gamma\gamma$ system,

$$\frac{\Delta N_{(e^+e^-\to e^+e^-\eta_c\to e^+e^-f)}}{\Delta W_{\gamma\gamma}}. \tag{7}$$

where f denotes one of the investigated decay modes. Given the detector efficiency $\mathcal{E}_f$, the integrated luminosity $\mathcal{L}$, and flux $L_{\gamma\gamma}$ of the two interacting photons parametrized by well known equivalent photon approximation formula, the invariant mass distribution can be converted into two-photon cross section multiplied by corresponding branching ratio:

$$\sigma_{\gamma\gamma\to\eta_c}(W_{\gamma\gamma})\cdot BR(\eta_c\to f) \;=\; \frac{\Delta N_{(e^+e^-\to e^+e^-\eta_c\to e^+e^-f)}}{\Delta W_{\gamma\gamma}\;\cdot\;\mathcal{L}\;\cdot\mathcal{E}_f(W_{\gamma\gamma})\;\cdot L_{\gamma\gamma}(W_{\gamma\gamma})} \tag{8}$$

The efficiency was calculated dividing bin-by-bin the simulated invariant mass distribution for events that passed all the cuts in the mass interval 2.5-4.0 $\mathrm{GeV/c^2}$ by the invariant mass distribution for the generated events. It should be noticed that both the $\gamma\gamma$ flux and the invariant mass efficiency distribution modify the background-to-signal ratio measured in the side-bands of the $\Delta N/\Delta W_{\gamma\gamma}$ distribution.

In order to determine the value of the η_c radiative width, the $\gamma\gamma$ invariant mass cross-section has been fitted to the Breit Wigner distribution of the form

$$BW(\Gamma_{\gamma\gamma}, M_{\eta_c}, \Gamma_{tot}, W_{\gamma\gamma}) = 8\pi(2J+1)\frac{\Gamma_{\gamma\gamma}\Gamma_{tot}}{(W_{\gamma\gamma}^2 - M_{\eta_c}^2)^2 + M_{\eta_c}^2\Gamma_{tot}^2} \tag{9}$$

describing the η_c production cross-section convoluted with a Gaussian mass resolution $G(W_{\gamma\gamma},\sigma)$ together with a background parametrization expressed in terms of polynomial function of the third order $P_3(W_{\gamma\gamma})$:

$$\sigma_{\gamma\gamma\to\eta_c}(W_{\gamma\gamma}) = [BW(\Gamma_{\gamma\gamma}, M_{\eta_c}, \Gamma_{tot}, W_{\gamma\gamma}) \;+\; P_3(W_{\gamma\gamma})] \otimes G(W_{\gamma\gamma},\sigma) \tag{10}$$

According to eq.(8) and eq.(9) the fit determines the product of the radiative width and the branching ratio, the mass of the resonance and the experimental mass resolution

σ. All these fitted parameters have been determined separately for each data sample because some of them explicitly depend on the energy (two-photon flux) and others on the period of the data collection (efficiency). The total width Γ_{tot} of the resonace has been fixed to value obtained by other experiments [19].

The width of the mass resolution distribution obtained from the above fit coincided within ±10% with that obtained from the simulated sample.

The final $\sigma_{\gamma\gamma}$ plots are average distributions from different samples. The resulting cross-sections multiplied by the corresponding branching ratios for $\eta_c \to K^0_s K^{\pm}\pi^{\mp}$, $\eta_c \to K^+K^-K^+K^-$ and $\eta_c \to K^+K^-\pi^+\pi^-$ are presented in Fig.6.

A major contribution to the systematic uncertainty originates from the cuts variation (about 44% of the total systematic error) and different fit ranges as well as the choice of binning (about 28%). Since both the branching ratio and $\Gamma_{\gamma\gamma}$ (see formula above) cannot be determined simultaneously, we have used branching ratios and corresponding uncertaintes obtained by other experiments, summarized in [19] . This sort of uncertainty also contributed to the total systematic error (in the amount of 13%). The remaining part of systematic error (15%) was due to the uncertaintes of background shape, trigger efficiency and integrated luminosity value.

In summary, the final values of the η_c radiative width for the three decay channels investigated are presented in Table 1:

final state	BR ($\eta_c \to final$ [19]) [%]	$N_{ev}(\eta_c)$	$\Gamma_{\gamma\gamma}$ [keV]
$K^0_s K^{\pm}\pi^{\mp}$	1.5±0.4	41	13.3 ± 2.6(stat.) ± 2.0(syst.) ± 3.5(BR)
$K^+K^-\pi^+\pi^-$	2.0±0.7	42	14.2 ± 4.9(stat.) ± 2.9(syst.) ± 4.9(BR)
$K^+K^-K^+K^-$	2.1±1.2	46	16.5 ± 4.3(stat.) ± 2.7(syst.) ± 9.4(BR)
$\pi^+\pi^-\pi^+\pi^-$	1.2±0.4	< 26	<5.5 at 95% confidence

Table 1: The branching ratios taken from PDG, the number of events and radiative widths for the particular decay modes. The $N_{ev}(\eta_c)$ is the number of events selected for region M_{η_c}± 150 MeV/c^2. In the case of four pions final state only an upper limit has been estimated assuming that all events in the η_c mass interval are background.

For the analysed channels, the results quoted above are the averages of the LEP1 and LEP2 results. The product $\Gamma_{\gamma\gamma}\cdot$ BR in the analysis of the four charged kaon decay channel is in agreement, within the large errors, with the result of the ARGUS Collaboration [10], which gives 0.231 ± 0.090 (stat.) ± 0.023 (syst.) keV.
A weighted mean of the radiative width value for the first three channels in Table 1 with weights inversely proportional to the total error squared has been determined.
The result is:

$$\Gamma_{\gamma\gamma}= 13.9 \pm 2.0(\text{stat.})\pm 1.4(\text{syst.})\pm 2.7(\text{BR})\ \text{keV}$$

Acknowledgements

We are greatly indebted to our technical collaborators, to the members of the CERN-SL Division for the excellent performance of the LEP collider, and to the funding agencies for their support in building and operating the DELPHI detector.
We acknowledge in particular the support of
Austrian Federal Ministry of Education, Science and Culture, GZ 616.364/2-III/2a/98,
FNRS–FWO, Flanders Institute to encourage scientific and technological research in the

industry (IWT), Federal Office for Scientific, Technical and Cultural affairs (OSTC), Belgium,
FINEP, CNPq, CAPES, FUJB and FAPERJ, Brazil,
Czech Ministry of Industry and Trade, GA CR 202/99/1362,
Commission of the European Communities (DG XII),
Direction des Sciences de la Matière, CEA, France,
Bundesministerium für Bildung, Wissenschaft, Forschung und Technologie, Germany,
General Secretariat for Research and Technology, Greece,
National Science Foundation (NWO) and Foundation for Research on Matter (FOM), The Netherlands,
Norwegian Research Council,
State Committee for Scientific Research, Poland, SPUB-M/CERN/PO3/DZ296/2000, SPUB-M/CERN/PO3/DZ297/2000 and 2P03B 104 19 and 2P03B 69 23(2002-2004)
JNICT–Junta Nacional de Investigação Científica e Tecnológica, Portugal,
Vedecka grantova agentura MS SR, Slovakia, Nr. 95/5195/134,
Ministry of Science and Technology of the Republic of Slovenia,
CICYT, Spain, AEN99-0950 and AEN99-0761,
The Swedish Natural Science Research Council,
Particle Physics and Astronomy Research Council, UK,
Department of Energy, USA, DE-FG02-01ER41155,
EEC RTN contract HPRN-CT-00292-2002.

References

[1] W.Kwong, J.L.Rosner and C.Quigg, Ann. Rev. Nucl. Sci. **37** (1987) 325; W.Kwong et al., Phys. Rev. **D37** (1988) 3210.
[2] E.S.Ackleh and T.Barnes, Phys. Rev. **D45** (1992) 232; L.J.Reinders, H.Rubinstein and S.Yazaki, Phys. Rep. **127-1** (1985) 1.
[3] PLUTO Collab., Ch.Berger et al., Phys.Lett. **B167** (1986) 120.
[4] MARKIII Collab., R.M.Baltrusaitis et al., Phys.Rev. **D33** (1986) 629.
[5] R704 Collab., C.Baglin et al., Phys.Lett. **B187** (1987) 191.
[6] TPC/2γ Collab., H.Aihara et al., Phys. Rev. Lett. **60** (1988) 2355.
[7] TASSO Collab., W.Braunschweig et all., Z.Phys. **C41** (1989) 533.
[8] CLEO Collab., W.Y.Chen et al., Phys.Lett. **B243** (1990) 169.
[9] DM2 Collab., D.Bisello et al., Nucl. Phys. **B350** (1991) 1.
[10] ARGUS Collab., H.Albrecht et al., Phys. Lett. **B338** (1994) 390.
[11] L3 Collab., M.Acciari et al., Phys. Lett. **B461** (1999) 155.
[12] CLEO Collab., G. Brandenburg et al. Phys. Rev. Lett. **85** (2000) 3095.
[13] DELPHI Collab., P. Aarnio et al., Nucl. Instr. and Meth. **A303** (1991) 233.
DELPHI Collab., P.Abreu et al., Nucl. Instr. and Meth. **A378** (1996) 57.
[14] V.Bocci et al., Nucl.Instr. and Meth. **A362** (1995) 361.
[15] The DELPHI Trigger Group, A. Augustinus et al. The DELPHI Trigger System at LEP2, CERN-EP/2002-086, accepted by Nucl. Instr. and Meth. A.
[16] H.Krasemann and J.A.M.Vermaseren, Nucl. Phys. **B184** (1981) 265.
[17] M.Poppe, Int. Journ. Modern Phys. **A1** (1986) 545.
[18] BES Collab, J. Z. Bai et al. hep-ex/0301004, Subm. to: Phys. Lett.**B**.
[19] D.E. Groom et al,(Particle Data Group) Eur. Phys. Jour. **C15** (2000) 1.

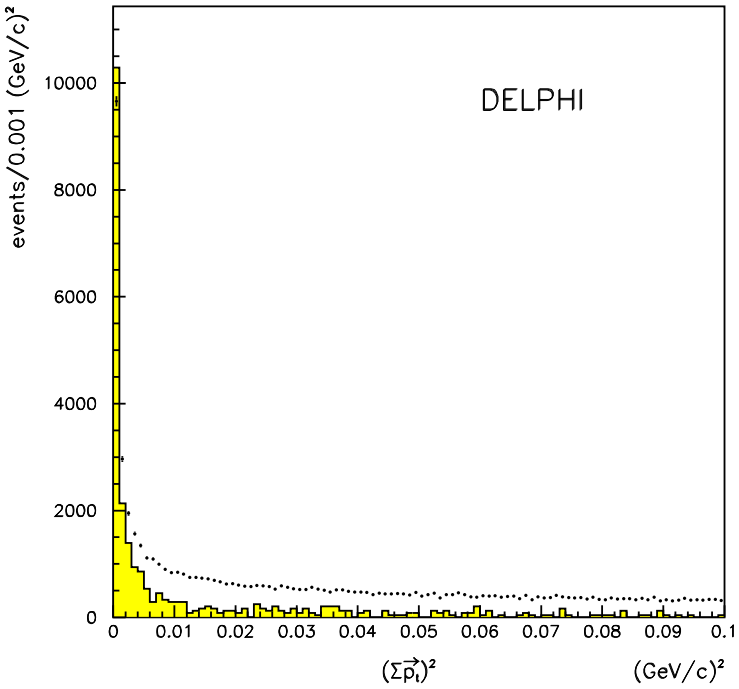

Figure 1: The square of the total transverse momentum of the hadronic system. Points represent the real data sample after the general data selection. The histogram shows this distribution for dedicated η_c production simulation sample with an arbitrary normalization.

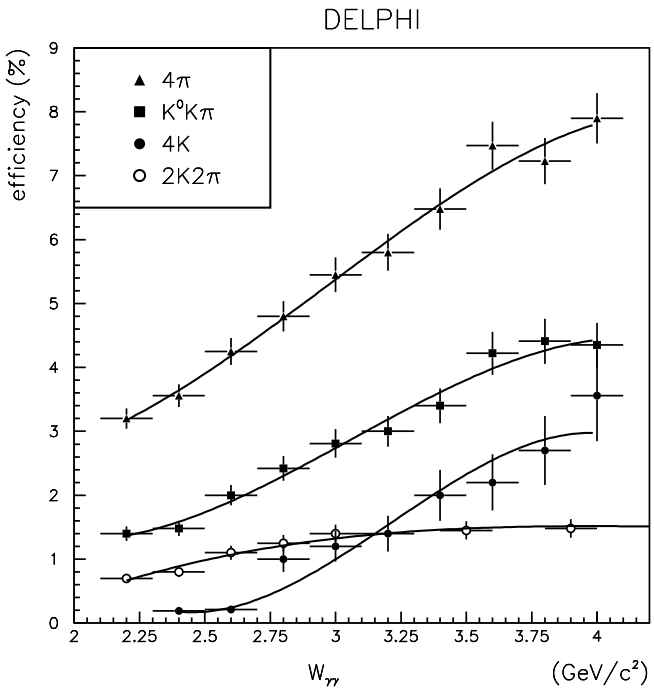

Figure 2: The average luminosity-weighted efficiences for different η_c decay final states as a function of the corresponding invariant mass. In the decay to K^0, its branching fraction to $\pi^+\pi^-$ has been taken into account.

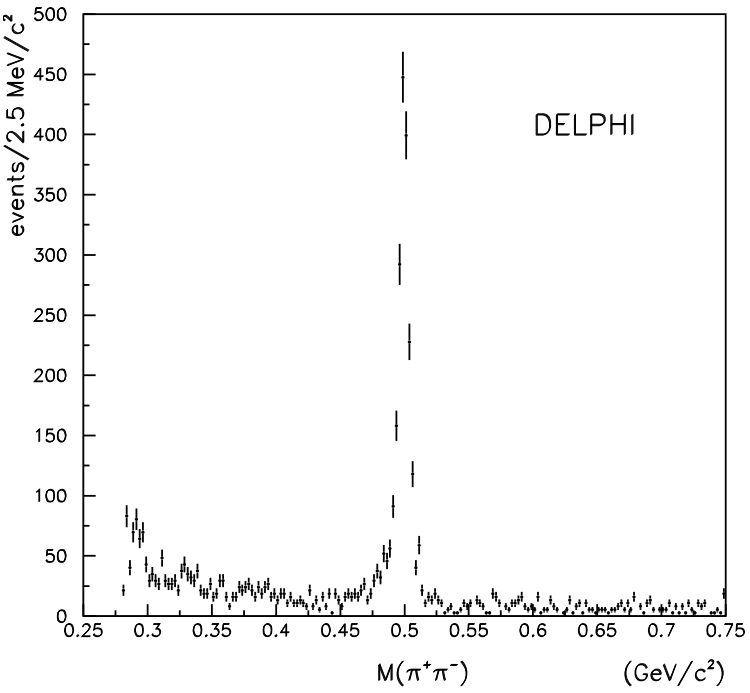

Figure 3: Invariant mass of two particles originating from a secondary vertex (summed over all energy samples).

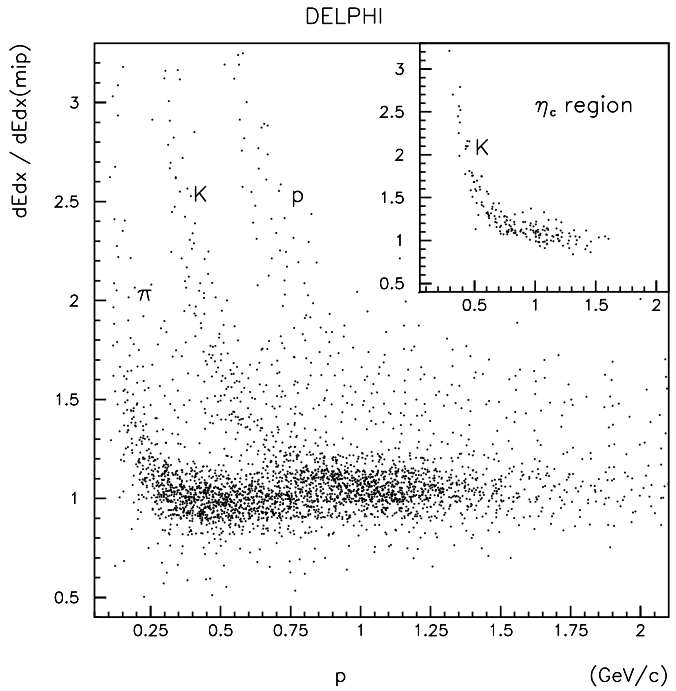

Figure 4: The dE/dx distribution for particles identified as a pion or a kaon in the data events after the general cuts. Most of the remaining tracks consist of protons. The same distribution for events from $\eta_c \to K^+K^-K^+K^-$ is shown in the insert.

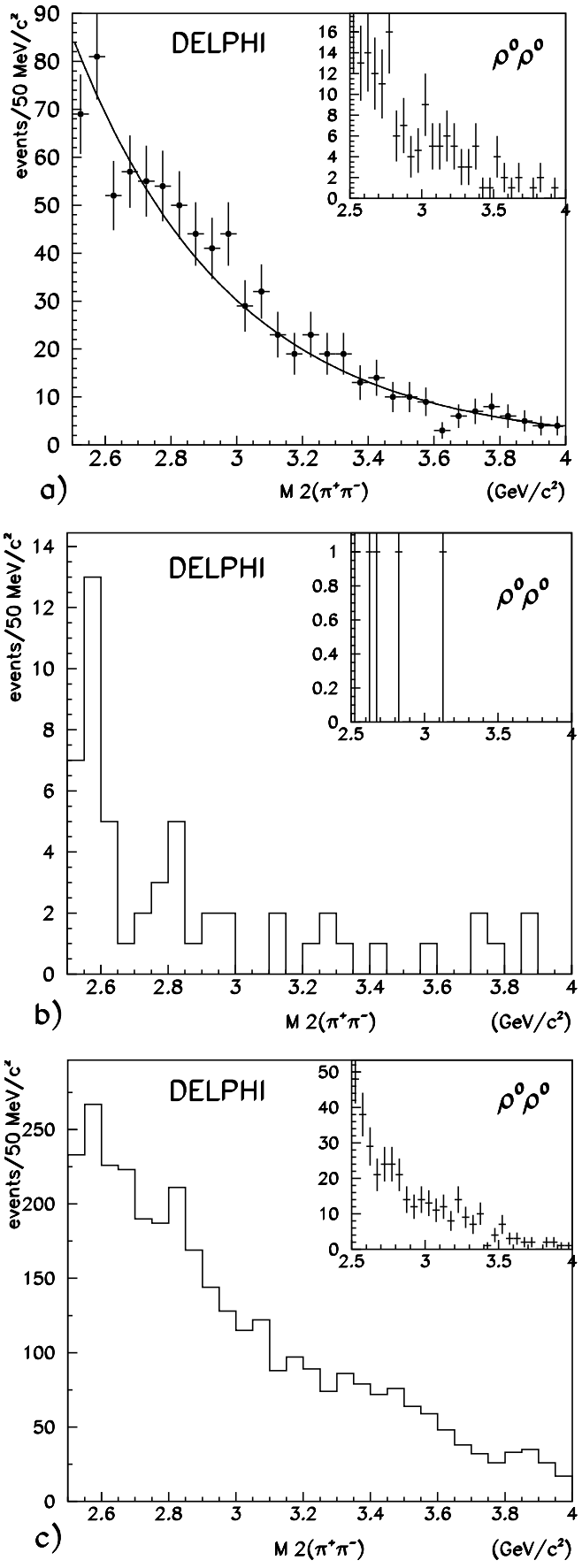

Figure 5: Final invariant mass distributions for the $\pi^+\pi^-\pi^+\pi^-$ decay final state. The presented distributions are based on: Fig.5a - the standard selection, Fig.5b - the stringent selection, Fig.5c - the looser selection, all of them described in the text. In the insets the

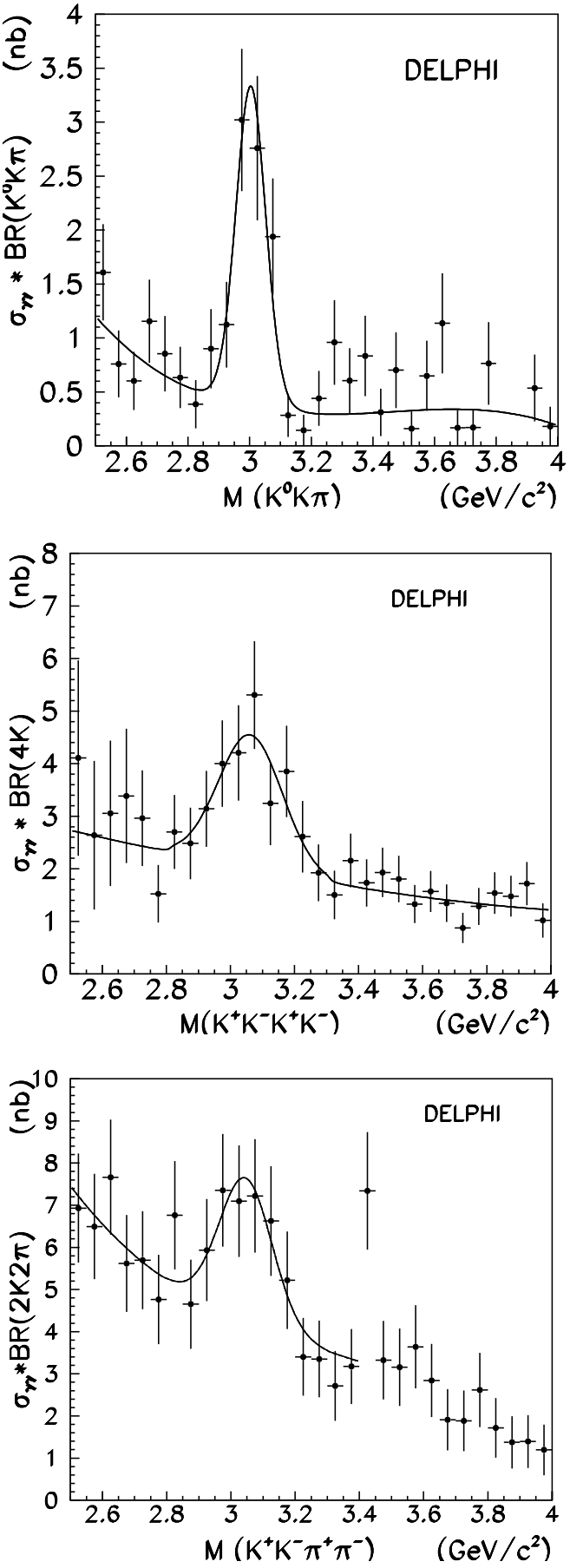

Figure 6: $\sigma(\gamma\gamma \to \eta_c)BR(\eta_c \to final)$. The curve shows the result of the fit described in the text.